Received 19 March 2021; revised 7 May 2021; accepted 17 May 2021. Date of publication 20 May 2021; date of current version 15 October 2021.
The review of this article was arranged by Editor S. K. Saha.

Digital Object Identifier 10.1109/JEDS.2021.3082420

Electrolyte-Gated Field Effect Transistors in Biological Sensing: A Survey of Electrolytes

GUAN YING WANG [1,2], KERYN LIAN [1], AND TA-YA CHU [2] (Senior Member, IEEE)

1 Materials Science and Engineering Department, University of Toronto, Toronto, ON M5S 3E4, Canada
2 Advanced Electronics and Photonics Research Centre, National Research Council Canada, Ottawa, ON K1A0R6, Canada

CORRESPONDING AUTHOR: G. Y. WANG (e-mail: jgy.wang@mail.utoronto.ca)

This work was supported by National Research Council Canada. The work of Guan Ying Wang was supported by Ontario Graduate Scholarship. The work of Keryn Lian was supported by NSERC Canada under Grant Discovery RGPIN-2016-06219.

ABSTRACT Low operating voltages, rapid response, and high-throughput fabrication compatibility are key advantages for the development of electrolyte-gated field effect transistors (EGFETs) for biological sensing. Among the key components in EGFET biosensors, electrolyte materials are relatively less investigated, especially alternatives to water-based liquid electrolytes such as ionic liquids, ion gels, polyelectrolytes, and solid polymer electrolytes. These electrolytes enable portable devices and environmental stability superior to their water-based liquid alternatives. In this review, we offer an up-to-date evaluation of the state of EGFET research and gauge the strengths and limitations of high-performance electrolytes for use in EGFET biosensor applications as well as the potential for computer-aided design of such sensing platforms. The recent progress of EGFET biosensors for some popular analytes are reviewed and the performance of these alternative electrolytes in transistor biosensing is assessed. The challenges and opportunities for electrolytes in EGFETs are discussed for future research directions in this field.

INDEX TERMS Biological sensing, electrolyte dielectrics, polymer electrolytes, printed electronics, thin film transistor.

I. INTRODUCTION

Electrolyte materials and electrolyte-gated field effect transistors (EGFETs) have gained attention for their printability, flexibility, and potential for large-scale manufacturing as well as their use in IoT devices, making them a promising option for emerging technologies such as artificial synapses [1]–[3], wearable electronics [4], [5], and biological sensing [6]–[8]. Different from a traditional organic thin film transistor that uses a layer of SiO_2 or polymer dielectric material, EGFETs use electrolytes – a liquid or solid-state ion-conducting material. Due to the high gating capacitance enabled by electrolyte materials, low-voltage operation of less than 1 V can be achieved, with enhanced portability.

Since the year 2000, there has been an interest in EGFET biosensors as shown in Fig. 1. After demonstrating that a thin film transistor (TFT) could be gated with just water [9], EGFETs have been seen as a viable option for sensing in body fluids. However, various challenges have emerged in the areas of device stability, printability, and large-scale manufacturing potential for aqueous devices. Alternative electrolytes like ionic liquids and solid or quasi-solid electrolytes such as ion gels, polyelectrolytes, and polymer electrolytes have emerged as materials with greater ambient stability, printability, and electrochemical performance, but further work is needed to identify compatible high-performance electrolytes for biosensors.

Once promising electrolytes for EGFET biosensors are identified, computer aided design will be indispensable in translating the biosensor into a mathematical model. This modeling will help determine the compatibility of the sensor components as well as guide experimental work and accelerate development while reducing trial and error.

The scope of this review is on EGFETs for biosensing applications focusing on the challenges and advantages of different types of electrolyte materials in EGFETs for biosensors. It is organized as follows:

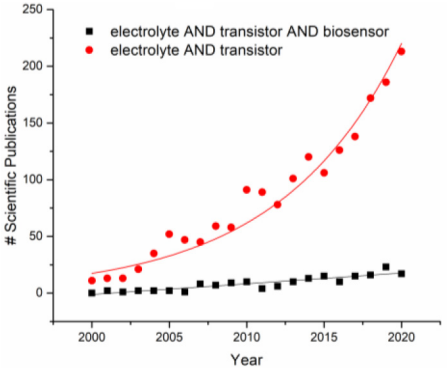

FIGURE 1. **This figure was obtained using the search terms "electrolyte AND transistor" and "electrolyte AND transistor AND biosensor" on Scopus. It shows an exponentially increase in the number of scientific publications reported on electrolyte transistors, and linearly increase in electrolyte transistor biosensors from the years 2000-2020 (as of December 10, 2020).**

Section II introduces the fundamental concepts related to biosensors and EGFETs;

Section III evaluates the merit of different electrolyte materials used in EGFETs;

Section IV discusses the achievements of EGFET biosensors so far;

Section V offers a perspective of the direction of development on electrolyte materials for transistor biosensors.

II. EGFET BIOSENSORS

A. BIOSENSOR BASIS AND COMPONENTS

The main components of the biosensor are a bio-recognition element, a transducer, and a signal processing unit [10]. A layer of bio-recognition elements is covalently attached to either the semiconductor or gate electrode interface, or less commonly on the substrate, in a surface functionalization step. For example, one method is to attach an enzyme to a carboxylated polyimide surface via a condensation reaction between an amine group on the enzyme and carboxylic acid [11].

The three main bio-recognition element types are complementary DNA pairings, antibody/antigen pairs, or enzyme/substrate pairs, which offer specific and selective binding of the target analyte to the bioreceptor as shown in Fig. 2. As the target analytes interact and bind with their recognition elements, certain changes in physical quantity of the transistor output will occur.

Some key FOM proposed by Picca *et al.* [12] for EGFET biosensors are the limit of detection (LOD), sensitivity, and dynamic range. The LOD is defined as the lowest amount of analyte discernible from a blank measurement with a confidence level of 99%, corresponding to 3 standard deviations from the mean measurement. The sensitivity is defined as the slope of a signal vs. concentration calibration curve covering at least 3 orders of magnitude [12]. The dynamic range is the concentration range over which a changing output signal is detected.

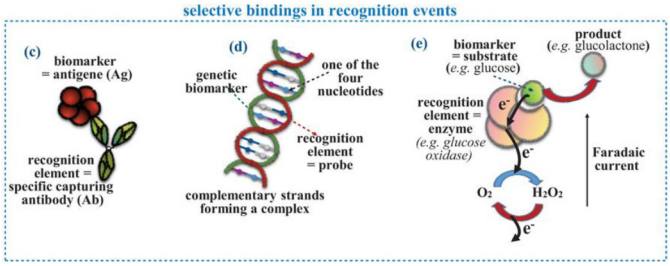

FIGURE 2. **Selective bindings in recognition events for complementary DNA pairings, antibody/antigen pairs, and enzyme/substrate pairs. Reprinted (adapted) with permission from [12]. Copyright 2020, Adv. Funct. Mater.**

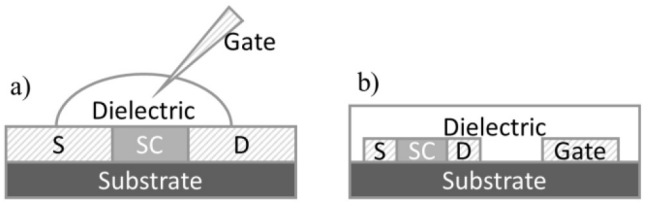

FIGURE 3. **Common EGFET architectures. a) Top gate bottom contact with liquid dielectric. b) Side gate, also known as in-plane or coplanar configuration.**

A key advantage of using an EGFET biosensor is that they are label-free. Unlike label-based biosensors which require an additional fluorescent or radioactive tag to quantify the presence of analytes, label-free biosensors detect analytes through the direct transduction of physical properties. This greatly reduces manufacturing complexity and cost. In addition, the use of an electrolyte dielectric provides a large capacitance to enable low-power operation, printability, and flexibility. Challenges for transistor biosensors lie in the sensing of only charged biomolecules, low reproducibility, and some limitations in sensing beyond the Debye length [13]–[15].

B. EGFET CONFIGURATIONS AND COMPONENTS

There are four general configurations: top gate bottom contact (TGBC), top gate top contact (TGTC), bottom gate bottom contact (BGBC), and bottom gate top contact (BGTC). There are various advantages in fabrication and performance when it comes to the types of configurations. When using liquid electrolytes, the dielectric may be a droplet on the surface of the semiconductor with a probe acting as a gate electrode immersed in the dielectric, as shown in Fig. 3a. Another common architecture is side-gate, where the source, drain, and gate electrodes are coplanar as shown in Fig. 3b.

C. EGFET OPERATION MECHANISM

When a bias is applied to the gate electrode, an electrical double layer (EDL) forms at the gate/electrolyte and semiconductor/electrolyte interfaces from the migration and accumulation of electrolyte ions according to the Stern-modified Gouy-Chapman double layer model. There is

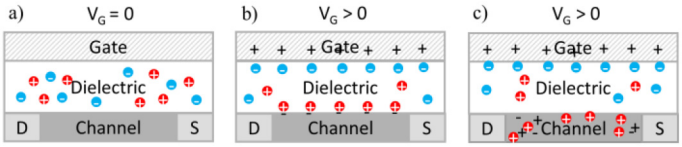

FIGURE 4. Thin film transistors that are a) unbiased b) biased EDLTs c) biased ECTs.

a Helmholtz layer at the immediate interface from an accumulated monolayer of ions, followed by the diffusion layer which has a high concentration of accumulated ions that decay exponentially with distance [16]. The EDLs can be considered as nanocapacitors with a thickness of approximately 1 nm. This small thickness permits high capacitance between 1-10 μF cm^{-2} at operating voltages of less than 2 V. The specific capacitance can be estimated by (1) [17]:

$$C = \frac{\kappa \epsilon_0}{\lambda} \tag{1}$$

where κ is the effective dielectric constant, ε_0 is the vacuum permittivity constant, and λ is the thickness of the EDL. The total EDL capacitance can be represented as the sum of the gate/electrolyte interface capacitance (C_{GE}) and the electrolyte/semiconductor interface capacitance (C_{ES}) as shown in (2). The gate/electrolyte capacitance is usually much higher than the electrolyte/semiconductor capacitance due to a larger contact area with the gate electrode. Thus, the capacitance of the latter dominates.

$$C_{EDL} = \left(C_{GE}^{-1} + C_{ES}^{-1} \right)^{-1} \tag{2}$$

The thickness of the EDL is known as the Debye screening length, the distance from the interface to the boundary between the diffusion and bulk layers. In the applications of biological sensing, the Debye length may limit the sensing distance of the receptor, as analytes beyond this length are shielded by ions in solution [18]. For this reason, a very concentrated solution or large or long receptor will cause detection issues [19]. However, sensing beyond the Debye length has been reported [20]–[22], which is desirable as high ionic concentrations are needed for large capacitances which simultaneously lower the Debye length. As reported by Palazzo *et al.* it is possible to obtain sensing many times beyond the Debye length with capacitive-controlled sensing at high salt concentrations [23]. Additional strategies for overcoming the Debye length have also been explored, including tuning the morphology of the channel, changing the design of the aptamer, and device modulation [19].

Fig. 4 illustrates the EDL formation mechanism for EGFETs. The unbiased state of the thin film transistor is shown in Fig. 4a. In the case that the semiconductor is impermeable under bias, a 2D EDL capacitor is formed at the interface when ions accumulate, resulting in high capacitance and low voltage operation, which dissipates when the bias is removed. These types of EGFETS are known as electrical double layer transistors (EDLTs). An example of an impermeable n-type transistor operating in accumulation mode is shown in Fig. 4b. In the case where the semiconductor can be penetrated under a bias, this electrochemical doping forms a 3D EDL. As the bias is removed, the channel de-dopes. These types of EGFETs are known as electrochemical transistors (ECTs). An example of a typical ECT operating in depletion mode is shown in Fig. 4c. Thus, the main difference between an EDLT and an ECT is the permeability of the channel. It should be noted that EDLTs may have some penetration of ions into the semiconductor, but the effects are minor compared to ECTs. In addition, as a gate bias is applied, the channel current for EDLTs is primarily modulated by the field effect, while the ECT channel current is modulated through the doping/de-doping of ions into the channel [24]. Although ECTs are well known in biological sensing applications due to their low voltage operation, high transconductance, and stable performance in aqueous environments [24], [25], this review focuses on the use of EDLTs due to their relative impermeability which reduces the degradation of the semiconductor, and their potential for solid-state, portable and flexible devices.

D. KEY FOM OF EGFETS

Some important indications of transistor performance are the ON-OFF current ratio (I_{ON}/I_{OFF}), mobility of the semiconductor, subthreshold swing, and OFF current. These are values that can be extracted from the voltage-current characteristics of the transistor. The drain current in the linear and saturated regions are expressed by (3) and (4):

$$I_{DS} = \frac{W}{L} \mu C (V_G - V_T) V_{DS} - \frac{{V_{DS}}^2}{2} \tag{3}$$

$$I_{DS} = \frac{W}{2L} \mu C (V_G - V_T)^2 \tag{4}$$

where I_{DS} is the drain current, W is the semiconductor channel width, L is the semiconductor channel length, μ is mobility, C is the specific capacitance of the dielectric, V_G is the gate voltage, and V_T is the threshold voltage.

III. DIELECTRICS USED IN EGFETS

A. AQUEOUS ELECTROLYTES

Aqueous electrolytes can form EDLs at the electrode interfaces with capacitances ranging from 0.9 - 3.8 μF cm^{-2} [9], [26], [27] which enable the transistors to operate at driving voltage <|0.5| V. To avoid cell rupture due to osmotic pressure, a salt solution or buffer is often used. Initially, the fabrication of a water-gated FET was demonstrated using deionized (DI) water with a reported specific capacitance of 3 μF cm^{-2} [9]. It was noted that the mobility of the rubrene semiconductor was lower than reported using SiO_2. Since water provides a larger capacitance, the charge carrier distribution is compressed more to the insulator/semiconductor interface, leading to a higher sensitivity to surface roughness and defects. It was then shown that a 0.2 M NaCl solution could be used to gate an organic device [26]. The mobility

of the organic semiconductor is comparable to the rubrene transistor described above due to its elongated alkyl chains forming a barrier at the water interface, preventing water penetration into the semiconductor.

There are several challenges and advantages for biological sensing. Aqueous electrolytes are not environmentally stable due to their fluid nature which hinders wearable solid-state device creation. However, this may be useful in a microfluidic sensing device which can be easily cleaned and disposed of. Their liquid state also allows receptors to be functionalized directly on the channel or gate of the transistor in a dense layer for higher sensitivity. Aqueous electrolytes can also have low conductivity, leading to slower EDL formation and slower switching speed [28]. For example, DI water can have conductivity as low as 5.5×10^{-5} mS cm^{-1}. Specifically for water-gated organic devices, the environmental instability of conjugated polymers such as P3HT in water lead to limited charge carrier mobility on the order of 10^{-3}. The low mobility may negate the advantage of high specific capacitance, reducing their useful usage in practical applications [26]. Adding salt may increase the ionic conductivity and increase the biological compatibility. However, this may cause ion penetration into the semiconductor layer, resulting in higher OFF current and reduced mobility, as well as hindering sensitive detection [27].

B. IONIC LIQUIDS (ILS)

ILs are defined as molten salts at room temperature, with a solvent-less composition of ions [29]. They are usually composed of nitrogen-containing organic cations and inorganic anions [30]. Due to their highly polar composition, high ionic conductivity, thermal and electrochemical stability, and non-volatility, they are attractive gate dielectric materials for EGFETs [30], [31]. Ionic diffusion can be in the range of 1 microsecond which translates to 1 MHz switching frequency [32], [33].

In 2008, Ono *et al.* demonstrated the fabrication of an IL-gated FET using a single crystal rubrene semiconductor [32]. Two similar devices were created using 1-ethyl-3-methylimidazolium bis (trifluoromethylsulfonyl) imide ([EMIM][TFSI]) and 1-ethyl-3methylimidazolium bis (fluorosulfonyl) imide ([EMIM][FSI]) IL. [EMIM][FSI] was shown to have a larger hysteresis than the [EMIM][TFSI]-gated device, attributed to the difference in interfacial interactions between the ionic liquid and semiconductor such as hole traps formed by impurities in the IL or absorption of moisture provided by the additional fluorine atoms.

In an example of a high-performance device, an extremely thin layer of IL, N,N-diethyl-N-methyl-N-(2-methoxyethyl) ammonium bis(trifluoromethanesulfonyl) imide ([DEME][TFSI]), was applied to electrostatically dope its MoS_2 semiconductor, resulting in a specific capacitance of 1.55 μF cm^{-2} and good device performance at low driving voltage [34].

Similar to aqueous electrolytes, ILs are limited by their fluid state. As a result of their liquid state, they also have lower resistance and may induce higher gate leakage current [35] from a combination of electrochemical reactions and absorption of environmental impurities such as water, nitrogen, and oxygen. Although generally considered stable, ILs have had unexpected reactions with other species in solution or at elevated temperatures [36]. Furthermore, there have been some environmental concerns with using fluorinated ILs. For example, [EMIM][TFSI] is a known toxin and environmental hazard, and [C4mim][PF6] is found to degrade to form hydrofluoric acid (HF) [37]. Thus, ILs may be hazardous and should be handled with care.

C. ION GELS

Ion gels are composed of a polymer matrix incorporated in an ionic liquid [38]. The polymer matrix can be chemically or physically crosslinked, and thus referred to as "chemical ion gels" or "physical ion gels". The IL acts as a plasticizing salt, and the resulting ion gel is a quasi-solid or solid-state composite electrolyte distinct from polymer gels due to their non-volatility. ILs in ion gels provide high ionic conductivity, low vapour pressure, as well as thermal and electrochemical stability [31]. In addition, they have a short polarization response time due to the decoupling of fast ion motion from polymer segmental motion [38] and high concentration of ionic species [39]. Mechanically supported by the polymer matrix, ion gels are a very promising electrolyte material for EGFETs.

C.1. PHYSICAL ION GELS

Triblock copolymers have been used as polymer matrices in ion gels due to their tunable structure and self-assembling capability. Cho *et al.* presented a high-performance fully printed ion gel gate dielectric transistor via aerosol jet [39]. The ion gel was a PS-PEO-PS triblock copolymer matrix self-assembled in [EMIM][TFSI] leading to a specific capacitance of approximately 20 μF cm^{-2} and an ionic conductivity of 8 mS cm^{-1}. The high ionic conductivity was attributed to the low gelation point of this physical self-assembled ion gel.

In an attempt to increase the electrical performance, Nketia-Yawson *et al.* demonstrated a high-performance solid-state electrolyte gate insulator (SEGI) made of poly(vinylidene difluoride-trifluoroethylene) (PVDF-TrFE) /poly(vinylidene fluoride-co-hexafluoropropylene) (PVDF-HFP)/[EMIM][TFSI] [40]. Their devices and performance can be seen in Fig. 5. In addition to edge-on orientation of the organic semiconductor enabling high mobility in the TGBC configuration, the good performance was also attributed to the high capacitance of up to 4.9 μF cm^{-2} provided by the SEGI and low contact resistance from the optimized device geometry.

C.2. CHEMICAL ION GELS

Chemical ion gels have been less developed due to more difficulties in controlling the crosslinking. To address this,

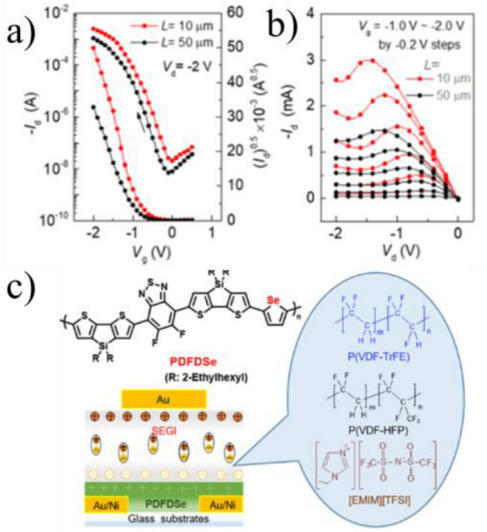

FIGURE 5. **The a, b) device performance and c) molecular structure, device configuration of SEGI EGFETs. Reprinted (adapted) with permission from [40]. Copyright 2018, Am. Chem. Soc.**

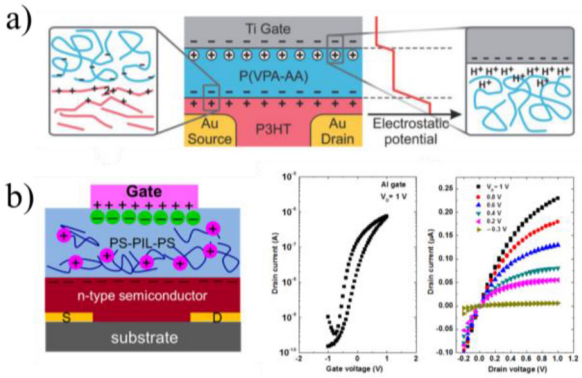

FIGURE 6. **a) Device configuration and chemical structure of polyelectrolyte EGFET. Reprinted (adapted) with permission from [54]. Copyright 2007, Adv. Mater. b) Device performance of single-ion conducting triblock copolymer polyelectrolyte. Reprinted (adapted) with permission from [51]. Copyright 2015, Am. Chem. Soc.**

Jeong *et al.* presented a chemically crosslinked, inkjet-printable self-assembling ion gel in EGFETs. The ion gel was composed of PVA polymer backbone, poly(ethyl methacrylate) (PEMA) chemical crosslinker, [EMIM][OTf] ionic species, and DMSO solvent [41]. The ion gel was reported to have a specific capacitance of 5.4 μF cm^{-2} and an ionic conductivity of 5 mS cm^{-1}. These printed transistors had excellent, stable performance between 20-90% relative humidity, because of the non-volatility of the ionic liquid [EMIM][OTf].

Generally, ion gels provide a high specific capacitance ranging between 1-31 μF cm^{-2} [39], [40], [42]–[49] and as large as 162 μF cm^{-2} [50] for low power operation; high ionic conductivities between 1-10 mS cm^{-1} also promote fast EDL formation. However, in addition to intrinsic properties of the electrolyte, excellent electrical performance also depends on material compatibility as well as a fabrication processes and geometry to optimize the overall performance of the devices.

D. POLYELECTROLYTES

Polyelectrolytes are polymers with ionizable groups in the backbone, where the small ions can dissociate and become mobile in solution [38]. Depending on the charge of the backbone group, polyelectrolytes can be polycations or polyanions. Polyacrylic acid (PAA) and polystyrene sulfonate (PSS)-based polyelectrolytes are common, with specific capacitances of approximately 10 μF cm^{-2}. A subcategory of polyelectrolytes are poly(ionic liquids) (PILs), which use ionic liquid instead of solid salt monomer. PILs have cationic or anionic centers in repeating units of the polymer chain. Overall, good mobility, large capacitance, and low OFF currents have been achieved, the I_{ON}/I_{OFF} ratio of the polyelectrolyte-gated devices and the ionic conductivity of these dielectric materials are often poor or unreported [51]–[56].

Herlogsson *et al.* presented a proton-conducting polyelectrolyte. The dielectric material used was P(VPA-AA), a random copolymer of vinyl phosphonic acid and acrylic acid, with a specific capacitance of 20 μF cm^{-2} [54]. The device configuration can be seen in Fig. 6a. Although the I_{ON}/I_{OFF} ratio of 140 is low, the electrolyte provided low voltage operation without electrochemical reactions in the semiconductor. This was possible due to the usage of large polyanionic chains that cannot penetrate the semiconductor, and the presence of protons naturally found in P(VPA-AA) to neutralize hydroxide from absorbed water which may penetrate the semiconductor.

An ion gel of polymerized ionic liquid triblock copolymer, PS-PIL-PS, composed of polystyrene and the polyionic liquid [EMIM][TFSI], with the cationic species [EMIM]$^+$polymerized into the backbone of the triblock copolymer was evaluated [51]. The device configuration and transfer and output curves for a typical device is displayed in Fig. 6b. An ionic conductivity of approximately 1×10^{-3} mS cm^{-1} and specific capacitance of approximately 1 μF cm^{-2} were obtained. The good electrical performance of this device and low hysteresis was due to limited ionic doping from bulky cation chains which prevented semiconductor degradation. In addition, the PS-PIL-PS was highly printable due to its mechanical robustness and hydrophobicity.

E. POLYMER ELECTROLYTES

Polymer electrolytes are ion-coordinating polymer matrices containing mobile ions [38]. Unlike polyelectrolytes, the mobile ions are not free in solution, but coupled to the polymer backbone. They are often cast or printed as solid or gel-like films, hence referred to as "solid polymer electrolytes" or "gel electrolytes". EDL formation is often slower and depends on the speed of segmental chain motion. The

TABLE 1. Summary of properties and performance of EGFET examples with different electrolytes.

Dielectric	Dielectric Material	C (μF cm^{-2})	σ (mS cm^{-1})	Configuration	S&D/G	Semiconductor	V_T	I_{ON}/I_{OFF}	μ (cm^2 V^{-1} s^{-1})
Water	Purified water [9]	3	N/A	TGBC	Au/Au	P3HT	-0.16	150	5.9×10^{-3}
Water	Purified water [9]	3	N/A	TGBC	Au/Au	Rubrene	-0.09	8×10^{4}	6.7×10^{-2}
Water	0.2 M NaCl [26]	0.9	N/A	TGBC	Au/W tip	PBTTT (non-annealed)	0	100	8×10^{-2}
Water	DI water [27]	3.8	N/A	TGBC	Au/Pt wire	TIPS-pentacene	-0.140	100	1.3×10^{-2}
DPBS	138 mM NaCl, other salts [27]	1.75	N/A	TGBC	Au/Pt wire	TIPS-pentacene	0.05	100	1.7×10^{-3}
IL	[EMIM][TFSI] [32]	11	20-30	TGBC	Au/Au wire	Single crystal rubrene	N/A	N/A	4.1×10^{-1}
IL	[EMIM][FSI] [32]	5.4	20-30	TGBC	Au/Au wire	Single crystal rubrene	N/A	N/A	1.2
IL	[DEME][TFSI] [34]	1.55	N/A	In-plane	Ti/Au	MoS_2	0.5	10^{7}	60
Ion gel	PVA, PEMA, [EMIM][OTf], DMSO [41]	5.4	5	TGBC	NR/PEDOT :PSS	In_2O_3	-0.138	1.3×10^{6}	N/A
Ion gel	P(VDF-TrFE)/P(VDF-HFP)/[EMIM][TFSI] [40]	4.9	N/A	TGBC	Au/Au	PDFDSe	-0.98	10^{5}	19.58
Polyelectrolyte	PS-PIL-PS, PIL = [EMIM][TFSI] [51]	1	N/A	TGBC	Au/Au	P(NDI2OD-T2)	0.4	2×10^{3}	8×10^{-3}
Polyelectrolyte	P(VPA-AA) [54]	20	N/A	TGBC	Au/Ti	P3HT	-0.29	140	1.2×10^{-2}
Polymer electrolyte	$LiClO_4$, PVA, PC, DMSO [57]	5.97	5.37	In-plane	ITO/ITO	In_2O_3	N/A	10^{6}	98.03
Polymer electrolyte	H_3PO_4, PVA [58]	3.09	0.08	In-plane	Au/Au	diF-TES-ADT: PS	-0.7	10^{5}	5

N/A: Not available in the literature.

ionic conductivity is in the range of 10^{-1} – 10^{-4} mS cm^{-1}, although recently developed electrolytes can have ionic conductivities of greater than 20 mS cm^{-1} [59], [60]. The low ionic conductivity is a concern resulting in slow switching time of the device. One longstanding and extensively studied example of a polymer electrolyte is PEO/$LiClO_4$ [61]–[63].

To improve the ionic conductivity, approaches such as adding another polymer to form a blend, adding plasticizing agents, or developing nanocomposites have been explored. Some groups have reported the fabrication of high performance printed transistors using a composite solid polymer electrolyte (CSPE) [64]–[66]. For example, Von Seggern *et al.* have shown that their CSPE, containing PVA polymer matrix, PC plasticizer, DMSO solvent, and $LiClO_4$ salt has good electrical performance in their device and a high ionic conductivity of 5.37 mS cm^{-1} as well as a specific capacitance of 5.97 μF cm^{-2} [57]. The advantage of using this CSPE is its good conformation to the rough surface of the semiconductor channel, enabling high capacitance gating [67]. In addition, the CSPE is mechanically robust and compatible with inkjet printing as well as forms a fast-drying film on which additional layers of different materials can be printed. The improvement in conductivity for the solid polymer electrolyte was attributed to plasticizer and solvent being trapped in the polymer, forming solvent channels for ions to travel, leading to fast EDL formation [68].

Aside from CSPEs, dielectrics based on biopolymers have also been reported with promising performance, desirable capacitance and ionic conductivity [69]–[72]. In addition, a proton-conducting H_3PO_4-PVA electrolyte has also been demonstrated with promising performance [58]. In general, the capacitance for these polymer electrolyte devices range from 0.93 to 40 μF cm^{-2}, with an I_{ON}/I_{OFF} ratio as large as 5×10^{6} [28], [57], [63], [67], [69]–[75]. While these polymer

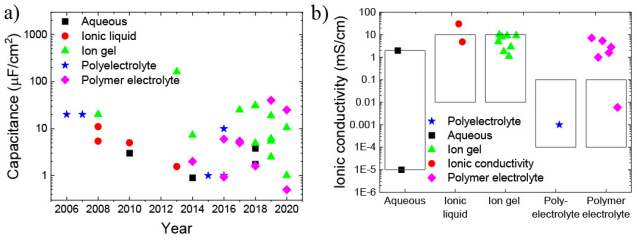

FIGURE 7. For aqueous, ionic liquid, ion gel, polyelectrolyte, and polymer electrolyte dielectrics, the a) specific capacitance and b) ionic conductivity.

electrolyte-gated FETs have high electrical performance, they are still susceptible to issues with temperature and moisture stability. Moving forward, the addition of additives may be crucial in optimizing high-performance polymer electrolytes.

F. SUMMARY OF ELECTROLYTES

Table 1 summarizes the transistor examples mentioned in Sections III A–E. Fig. 7a shows the range of specific capacitances for different types of electrolytes in EGFETs over the years. Even as early as 2006, electrolyte materials with capacitances greater than 10 μF cm^{-2} were reported. Ion gels and polymer electrolytes are mostly in the recent years and the highest specific capacitance values is up to 162 μF cm^{-2}, which is three to four orders of magnitude higher than the common dielectric material, such as SiO_x and PVP in OTFTs.

Fig. 7b shows the ionic conductivities between the different types of electrolytes as well as DI water (ca. 5.5×10^{-5} mS cm^{-1}) and PBS (ca. 3 mS cm^{-1}) [17], [76]. The ionic conductivity of ILs was found to be in a large range between 1 and 30 mS cm^{-1} [32], [77]. The ionic conductivity of polymer electrolytes is usually reported to be ranging from ca. 10^{-4} to 10^{-1} mS cm^{-1} [38], [78],

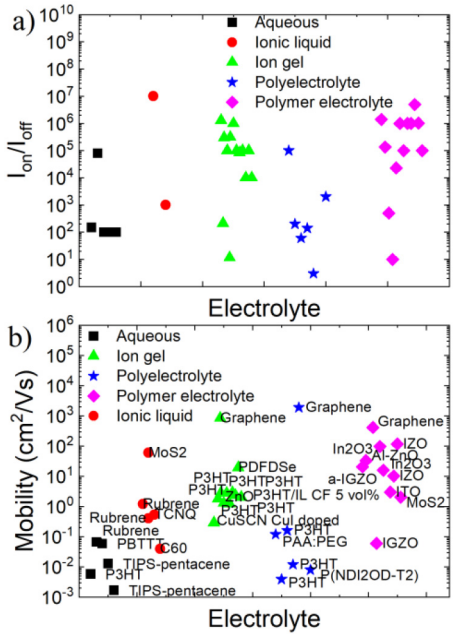

FIGURE 8. **For aqueous, ionic liquid, ion gel, polyelectrolyte, and polymer electrolyte dielectrics, the a) I_{ON}/I_{OFF} ratio and b) the majority carrier mobility.**

but some recent work reports higher ionic conductivity of approximately 20 mS cm^{-1} [59], [60]. Although ionic conductivity is an important factor affecting EDL formation time and device performance, a significant portion of papers reporting transistor performance did not include them. It is highly recommended to report ionic conductivity of the electrolyte when presenting transistor performance to help the community identify potential high-performance materials.

Fig. 8a shows the I_{ON}/I_{OFF} ratio for different types of electrolyte-gated transistors. The I_{ON}/I_{OFF} ratio for liquid-state electrolytes were generally around 100 and below 10^3 for polyelectrolytes. Those for ion gels and polymer electrolytes were among some of the highest, mostly between 10^4-10^6.

The reported mobility of the majority carriers from the literature is shown in Fig. 8b for the EGFETs classified based on the type of electrolyte. It is not surprising that 2D materials like graphene and MoS_2 consistently give high mobility regardless of the type of electrolyte used, and that the mobility of P3HT is mostly consistent, especially within electrolyte types. It is also noted that polymer electrolytes mainly use inorganic while the rest use organic semiconductors. One reason for this could be the incompatibility of inorganic semiconductors with certain device configurations. For example, BGTC devices have a semiconductor layer deposited after the polymer electrolyte layer which may damage the polymer electrolytes if annealing of the semiconductor is required. Another reason might be that these devices are focusing on the high mobility and performance of inorganic semiconductors, where low-temperature processing and flexibility are less of a concern.

In addition to the survey of the figures for capacitance, ionic conductivity, and I_{ON}/I_{OFF} ratio, a qualitative assessment of the performance of electrolyte materials for EGFETs was performed based on five performance and processing criteria as a radar graph in Fig. 9. In the graph, 5 types of electrolyte are analyzed for their: 1) specific capacitance, 2) ionic conductivity, 3) ease of synthesis, 4) environmental stability, and 5) printability/compatibility with printing technology.

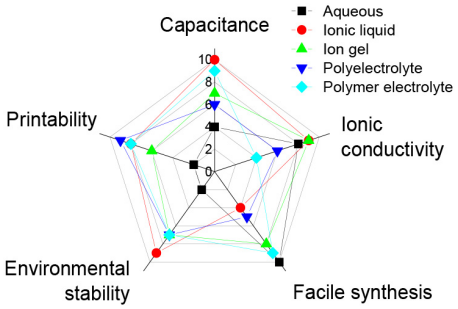

FIGURE 9. **Qualitatively assessed electrolyte performance in terms of capacitance, ionic conductivity, ease of synthesis, environmental stability, and printability.**

Aqueous electrolytes have the advantages of high ionic conductivity and facile synthesis, but lower capacitances, poor compatibility with printing fabrication techniques and low environmental stability due to their evaporation. Ionic liquids, while possessing high capacitance, ionic conductivity, and environmental stability as well as good printability, are not easily synthesized and are more expensive to produce. Ion gels are well-balanced, with good capacitance and ionic conductivity, and often simple but time-consuming synthesis procedures. They are more environmentally stable than aqueous electrolytes, but are still susceptible to changes in humidity and temperature. They are also compatible with printing processes, but less so than polyelectrolytes. Polyelectrolytes possess high printability and environmental stability, but have mediocre capacitance, ionic conductivity, and a complicated synthesis depending on the type of material. Finally, polymer electrolytes boast high printability. Similar to ion gels, they often have simple but time-consuming fabrication. They have excellent capacitance and acceptable ionic conductivity, and possess higher environmental stability than aqueous electrolytes but less than that of ionic liquids.

IV. BIOLOGICAL SENSING

Currently, most electrolytes applied in EGFET for biological sensing are aqueous as depicted in Fig. 10a with less than 10% employing non-aqueous electrolytes. The most common aqueous electrolyte is phosphate-buffered saline (PBS), which accounts for almost 70% of the electrolytes among over 50 papers surveyed. Aside from PBS, numerous other examples of aqueous electrolytes include DI water [79]–[82], salt solutions such as KCl/HEPES [83], and other cell culture mediums such as mTeSR [84], Dulbecco's modified Eagle's medium [85], or Bold's basal medium [7].

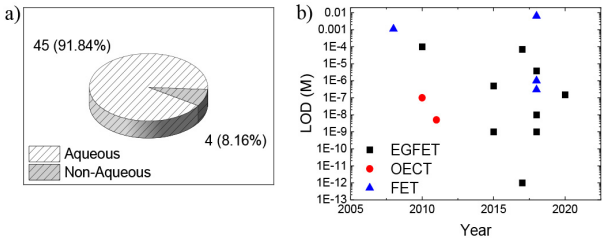

FIGURE 10. a) Comparing the percentage of aqueous-based and non-aqueous based electrolyte dielectrics in the literature surveyed. b) LODs reported for glucose EGFET, OECT, FET biosensors from the years 2008-2020.

A. GLUCOSE BIOSENSING

One of the most popular biological sensing applications is glucose sensing. A common operating mechanism for the sensing of glucose is the utilization of the enzyme-substrate pair of glucose oxidase (GOx) and glucose. GOx is covalently attached to the channel surface. As glucose is captured and oxidized, H_2O_2 is produced, which decomposes under the applied bias to yield electrons. The electrons are transferred to the gate electrode and results in a drop in potential across the gate electrode, which is transduced and recorded. This mechanism is shown in (4) and (5) [86]:

$$glucose + O_2 \xrightarrow{GOx} gluconolactone + H_2O_2 \quad (5)$$

$$H_2O_2 \rightarrow O_2 + 2H^+ + 2e^- \quad (6)$$

Most of the reported EGFET and OECT glucose biosensors used PBS liquid electrolyte [11], [44], [86]–[92]. Notably, an exception that uses a non-water-based electrolyte dielectric is an OECT by Yang *et al.*, which incorporates room temperature IL, triisobutyl-(methyl)-phosphonium tosylate ($[P_{1,4,4,4}][Tos]$), for label-free glucose sensors [29]. The IL acts as a reservoir for the redox enzyme glucose oxidase (GOx) and mediator ferrocene. When PBS is added, the IL is dissolved and allows all components to interact. The OECT obtained a LOD of 10^{-7} M and a dynamic range spanning 10^{-7} to 10^{-2} M.

Fig. 10b summarizes the LODs reported for various EGFET glucose biosensors alongside those of OECTs and FETs. In general, EGFETs were able to match and outperform OECT and FET devices, with an LOD as low as 1 pM [11]. Typical glucose levels in body fluids are tens of mM for blood, under 0.6 mM for sweat, and under 0.08 mM for saliva [93]. Thus, the LODs reported for EGFETs are acceptable for detection in a variety of body fluids, not just blood. Commercial glucose tests from major companies, which typically use electrochemical sensing, were reported to have detection ranges between 0.6 and 33 mM [94]. This is suitable for their intended use in blood glucose tests but are not sensitive enough for other body fluids. Thus, electrochemical sensors are currently being developed to meet the sensing requirements for other fluids such as sweat [95]. Furthermore, the accuracy of commercial glucose monitoring test strips was reported to not yet meet the necessary ISO criteria [93], [96], suggesting a need for further development of glucose biosensors in order to increase the accuracy and stability of the commercial product.

B. CORTISOL BIOSENSING

Another popular biological sensing application is cortisol detection. Cortisol is a stress biomarker found in various bodily fluids. Due to the association between stress and health, it is an important biomarker in health diagnostics. The gate dielectric is commonly PBS [97]–[99] and the LOD can be as low as 1 pM [99]. A stacked dielectric EGFET device structure has been developed by Massey *et al.* for the sensing of complex biofluids such as cortisol in saliva [100] without using PBS. They demonstrated the fabrication of a TGBC structure where the PMMA, Teflon coating, and cortisol aptamer-functionalized biofilm stack can be considered as the gate dielectric. Compared to a conventional EGFET, the advantages are a fast response time of 1 ms, selectivity in the presence of cortisone and progesterone, resistance to changes in bulk conductivity and dielectric permittivity, and reliable response to changes in concentration. The LOD and dynamic ranges of this device had comparable performance to conventional cortisol biosensors.

C. NEUROTRANSMITTER BIOSENSING

Another promising application is neurotransmitter detection of serotonin [101], dopamine [102], [103], and acetylcholine [104], [105]. LODs in EGFETs as low as 1 pM [102] have been reported for dopamine which outperform FET and OECTs [106]–[109]. A notable example of dopamine sensing is presented by Massey *et al.*, using a stacked dielectric reusable device with a fast response time on the order of 1 μs [110].

D. LIMITATIONS IN SOLID-STATE ELECTROLYTE-GATED BIOSENSORS

While there have been many studies on aqueous electrolyte-gated biosensors, research on solid-state electrolyte-gated biosensors is sparse. Issues may lie in the integration of solid-state electrolytes with biosensor receptors, or lack of exploration in the relatively new field of solid-state materials for EGFETs. There are still many efforts in detecting different target analytes in water-based liquids. So far, almost all examples not using water-based liquid electrolytes have been in floating or back gate EGFETs or OECTs which provides a simple setup and mimics human body fluid conditions. However, there may be lower sensitivity from limited diffusive transport in the aqueous media.

Two notable examples of biosensor EGFETs not using water-based liquid electrolytes are for ricin [111] and Cdk5 [112] which separate the "sensing" and "transducing" components of the transistor biosensor to reap the benefit of having aqueous biosensing as well as sensitive transduction. In the former example, a floating gate transistor was applied for the label-free detection of ricin in complex media with a flow-based microfluidic setup [111].

Polystryene-b- methylmethacrylate-stryene (SMS)/[EMIM][TFSI] ion gel was used. One arm of the floating gate was coupled to a control gate using an aqueous electrolyte for transduction. The other arm of the floating gate was functionalized with ricin-specific DNA aptamers as the capture surface. From the transfer curve, an I_{ON}/I_{OFF} ratio of approximately 10^6 and an OFF current of 10^{-10} A was extracted. The device had a LOD of 30 pM (1 ng/mL) in PBS buffer and 300 pM (10 ng/mL) in orange juice, which is within the LD_{50} of approximately 20 μg/kg for ricin.

V. CONCLUSION AND PERSPECTIVES

This review focuses on the applications of electrolytes in EGFETs as well as EGFET enabled biosensors. Many electrolytes used in EGFETs also have characteristics advantageous to biological sensing. Five types of electrolytes were analyzed for their strengths and weaknesses as follows:

- Aqueous electrolytes are the current preferred electrolytes for gating due to their compatibility with biological analytes, resemblance to biological fluids, simple synthesis and testing procedures, as well as standardized composition, but are not environmentally stable which limits their use in portable or wearable biosensors;
- Ionic liquids have high stability, but are susceptible to the same limitations as aqueous electrolytes due to their liquid nature. In addition, their difficult synthetic processes and higher cost may be limiting factors in large-scale manufacturing of disposable devices;
- Ion gels can improve the issues in ionic liquids while maintaining high performance, and good compatibility with printing technologies which enables high-throughput manufacturing and portable devices;
- Polyelectrolytes have high printability but poor ionic conductivity. One important challenge for these materials is their susceptibility to the environment. The devices are recommended to be encapsulated;
- Polymer electrolytes can have high performance, and portable withsimple processability and printability, albeit may need lengthy synthesis.

Considering the parameters of cost, printability, and large-scale manufacturing, one key issue that limits the all-printed fabrication of EGFETs is a shortage of compatible electrodes. Currently, the standard electrode is gold, fabricated through sputtering or evaporation. Although gold nanoparticle ink is commercially available, it is too expensive for mass manufacturing. Silver nanoparticle ink is a much cheaper alternative, but silver has compatibility issues with most electrolytes due to oxidation or corrosion. In order to realize all-printed, disposable, and low-cost devices, a suitable printable electrolyte material for transistors must be realized.

Another issue for EGFETs is their stability. Materials selection and transistor design are highly influential in determining the stability of an EGFET. Many approaches have been used for improving the stability of TFTs so far: the addition of additives [68], fine-tuning the composition of a component [113], encapsulation [114], barriers [51], or modification of the transistor geometry [115]. Further exploration is needed, especially to control the temperature, humidity, and electrochemical stability of EGFETs.

In biosensing, a majority of the published work focuses on expanding analyte detection and improving the FOM such as LOD, dynamic range, sensitivity, signal-to-noise ratio, and selectivity. There is less emphasis on how the component materials of the biosensor can be integrated and optimized, so the use of water-based liquids to complete a proof of concept for the device is sufficient. In non-water-based liquids, solids, and quasi-solids the receptors cannot be functionalized directly on the channel or gate and covered by the gating electrolyte. However, these non-water electrolytes are significantly more stable and possess better electrochemical performance. Once promising electrolytes are identified, computer-aided design will become important for accelerating the development of both high-performance devices and integrated circuits in biosensing. The compact model, for example, can be a tool that bridges the device development and incorporation into integrated circuits for practical applications. Using a compact model, the cost and time required from trial and error will be greatly reduced. For example, compact models have been developed for inorganic [116], organic [117], [118], and electrolyte-gated [119] FETs. In the future, using a device architecture that separates the "sensing" and "transducing" parts of the EGFET may become a viable strategy to achieve high sensitivity, selectivity, and stability for biosensors.

Overall, while aqueous electrolytes are indisputably the current majority for EGFET biosensing, ion gels and polymer electrolyte devices are promising in their high capacitance, high ionic conductivity, facile synthesis, and printability for disposable, mass-manufactured, flexible, and portable biosensors. Current EGFETs have been incorporated into printed circuits [120], [121]. In the future, fully printed devices and integrated sensors can be expected, especially with the aid of computer-aided design. In addition, the stability of these electrolytes must be improved to increase their compatibility in EGFET for biosensor applications to meet the requirements for next generation of portable and wearable biosensing platforms.

REFERENCES

[1] X. Li *et al.*, "Multi-terminal ionic-gated low-power silicon nanowire synaptic transistors with dendritic functions for neuromorphic systems," *Nanoscale*, vol. 12, no. 30, pp. 16348–16358, 2020, doi: 10.1039/d0nr03141k.

[2] G. Lu, Y. Liu, F. Lin, K. Gen, W. Wu, and R. Yao, "Realization of artificial synapse and inverter based on oxide electric-double-layer transistor gated by a chitosan biopolymer electrolyte," *Semicond. Sci. Technol.*, vol. 35, no. 7, pp. 75014–75025, 2020, doi: 10.1088/1361-6641/ab883e.

[3] R. Garcia-Cortadella *et al.*, "Distortion-free sensing of neural activity using graphene transistors," *Small*, vol. 16, no. 16, Apr. 2020, Art. no. 1906640, doi: 10.1002/smll.201906640.

[4] Q. Zhang, F. Leonardi, R. Pfattner, and M. Mas-Torrent, "A solid-state aqueous electrolyte-gated field-effect transistor as a low-voltage operation pressure-sensitive platform," *Adv. Mater. Interfaces*, vol. 6, no. 16, pp. 1–8, 2019, doi: 10.1002/admi.201900719.

[5] I. Babeli, G. Ruano, J. Casanovas, M. P. Ginebra, J. García-Torres, and C. Alemán, "Conductive, self-healable and reusable poly(3,4-ethylenedioxythiophene)-based hydrogels for highly sensitive pressure arrays," *J. Mater. Chem. C*, vol. 8, no. 25, pp. 8654–8667, 2020, doi: 10.1039/d0tc01947j.

[6] S. K. Sailapu *et al.*, "Standalone operation of an EGOFET for ultra-sensitive detection of HIV," *Biosens. Bioelectron.*, vol. 156, pp. 1–7, May 2020, doi: 10.1016/j.bios.2020.112103.

[7] J. Le Gall *et al.*, "Monitoring photosynthetic microorganism activity with an electrolyte-gated organic field effect transistor," *Biosens. Bioelectron.*, vol. 157, pp. 956–5663, Jun. 2020, doi: 10.1016/j.bios.2020.112166.

[8] E. Macchia *et al.*, "Single-molecule detection with a millimetre-sized transistor," *Nat. Commun.*, vol. 9, no. 1, p. 3223, 2018, doi: 10.1038/s41467-018-05235-z.

[9] L. Kergoat *et al.*, "A water-gate organic field-effect transistor," *Adv. Mater.*, vol. 22, no. 23, pp. 2565–2569, 2010, doi: 10.1002/adma.200904163.

[10] Y.-C. Syu, W.-E. Hsu, and C.-T. Lin, "Review—Field-effect transistor biosensing: Devices and clinical applications," *ECS J. Solid-State Sci. Technol.*, vol. 7, no. 7, pp. Q3196–Q3207, 2018, doi: 10.1149/2.0291807jss.

[11] S. Joshi, V. D. Bhatt, H. Wu, M. Becherer, and P. Lugli, "Flexible lactate and glucose sensors using electrolyte-gated carbon nanotube field effect transistor for non-invasive real-time monitoring," *IEEE Sensors J.*, vol. 17, no. 14, pp. 4315–4321, Jul. 2017, doi: 10.1109/JSEN.2017.2707521.

[12] R. A. Picca *et al.*, "Ultimately sensitive organic bioelectronic transistor sensors by materials and device structure design," *Adv. Funct. Mater.*, vol. 30, no. 20, May 2020, Art. no. 1904513, doi: 10.1002/adfm.201904513.

[13] Q. Fan *et al.*, "Solution-gated transistors of two-dimensional materials for chemical and biological sensors: Status and challenges," *Nanoscale*, vol. 12, no. 21. pp. 11364–11394, 2020, doi: 10.1039/d0nr01125h.

[14] T. Sakata, "Biologically coupled gate field-effect transistors meet in vitro diagnostics," *ACS Omega*, vol. 4, no. 7, pp. 11852–11862, 2019, doi: 10.1021/acsomega.9b01629.

[15] M. Kaisti, "Detection principles of biological and chemical FET sensors," *Biosens. Bioelectron.*, vol. 98, pp. 437–448, Dec. 2017, doi: 10.1016/j.bios.2017.07.010.

[16] K. B. Oldham, "A Gouy-Chapman-Stern model of the double layer at a (metal)/(ionic liquid) interface," *J. Electroanal. Chem.*, vol. 613, no. 2, pp. 131–138, 2008, doi: 10.1016/j.jelechem.2007.10.017.

[17] S. H. Kim *et al.*, "Electrolyte-gated transistors for organic and printed electronics," *Adv. Mater.*, vol. 25, no. 13, pp. 1822–1846, 2013, doi: 10.1002/adma.201202790.

[18] E. Stern, R. Wagner, F. J. Sigworth, R. Breaker, T. M. Fahmy, and M. A. Reed, "Importance of the debye screening length on nanowire field effect transistor sensors," *Nano Lett.*, vol. 7, no. 11, pp. 3405–3409, 2007, doi: 10.1021/nl071792z.

[19] Z. Zheng, H. Zhang, T. Zhai, and F. Xia, "Overcome debye length limitations for biomolecule sensing based on field effective transistors†," *Chin. J. Chem.*, vol. 39, no. 4, pp. 999–1008, 2021, doi: 10.1002/cjoc.202000584.

[20] C. H. Chu *et al.*, "Beyond the Debye length in high ionic strength solution: Direct protein detection with field-effect transistors (FETs) in human serum," *Sci. Rep.*, vol. 7, no. 1, p. 5256, 2017, doi: 10.1038/s41598-017-05426-6.

[21] G. S. Kulkarni and Z. Zhong, "Detection beyond the Debye screening length in a high-frequency nanoelectronic biosensor," *Nano Lett.*, vol. 12, no. 2, pp. 719–723, Feb. 2012, doi: 10.1021/nl203666a.

[22] M. Magliulo *et al.*, "Electrolyte-gated organic field-effect transistor sensors based on supported biotinylated phospholipid bilayer," *Adv. Mater.*, vol. 25, no. 14, pp. 2090–2094, 2013, doi: 10.1002/adma.201203587.

[23] G. Palazzo *et al.*, "Detection beyond Debye's length with an electrolyte-gated organic field-effect transistor," *Adv. Mater.*, vol. 27, no. 5, pp. 911–916, 2015, doi: 10.1002/adma.201403541.

[24] P. Lin and F. Yan, "Organic thin-film transistors for chemical and biological sensing," *Adv. Mater.*, vol. 24, no. 1, pp. 34–51, 2012, doi: 10.1002/adma.201103334.

[25] D. Khodagholy *et al.*, "High transconductance organic electrochemical transistors," *Nat. Commun.*, vol. 4, pp. 1–6, Jul. 2013, doi: 10.1038/ncomms3133.

[26] R. Porrazzo, S. Bellani, A. Luzio, E. Lanzarini, M. Caironi, and M. R. Antognazza, "Improving mobility and electrochemical stability of a water-gated polymer field-effect transistor," *Org. Electron.*, vol. 15, no. 9, pp. 2126–2134, 2014, doi: 10.1016/j.orgel.2014.06.002.

[27] N. Lago *et al.*, "TIPS-pentacene as biocompatible material for solution processed high-performance electronics operating in water," *IEEE Electron Device Lett.*, vol. 39, no. 9, pp. 1401–1404, Sep. 2018, doi: 10.1109/LED.2018.2856462.

[28] B. J. Kim, S. H. Um, W. C. Song, Y. H. Kim, M. S. Kang, and J. H. Cho, "Water-gel for gating graphene transistors," *Nano Lett.*, vol. 14, no. 5, pp. 2610–2616, May 2014, doi: 10.1021/nl500446s.

[29] S. Y. Yang *et al.*, "Electrochemical transistors with ionic liquids for enzymatic sensing," *Chem. Commun.*, vol. 46, no. 42, pp. 7972–7974, Nov. 2010, doi: 10.1039/c0cc02064h.

[30] R. Misra, M. McCarthy, and A. F. Hebard, "Electric field gating with ionic liquids," *Appl. Phys. Lett.*, vol. 90, no. 5, 2007, Art. no. 52905, doi: 10.1063/1.2437663.

[31] M. A. B. H. Susan, T. Kaneko, A. Noda, and M. Watanabe, "Ion gels prepared by in situ radical polymerization of vinyl monomers in an ionic liquid and their characterization as polymer electrolytes," *J. Amer. Chem. Soc.*, vol. 127, no. 13, pp. 4976–4983, 2005, doi: 10.1021/ja045155b.

[32] S. Ono, S. Seki, R. Hirahara, Y. Tominari, and J. Takeya, "High-mobility, low-power, and fast-switching organic field-effect transistors with ionic liquids," *Appl. Phys. Lett.*, vol. 92, no. 10, 2008, Art. no. 103313, doi: 10.1063/1.2898203.

[33] T. Uemura, M. Yamagishi, S. Ono, and J. Takeya, "Very low-voltage operation of ionic liquid-gated n-type organic field-effect transistors," *Jpn. J. Appl. Phys.*, vol. 49, no. 1, 2010, Art. no. 01AB13, doi: 10.1143/JJAP.49.01AB13.

[34] M. M. Perera *et al.*, "Improved carrier mobility in few-layer MoS2 field-effect transistors with ionic-liquid gating," *ACS Nano*, vol. 7, no. 5, pp. 4449–4458, 2013, doi: 10.1021/nn401053g.

[35] J. Seidemann, *Iontronics—Field Effect Study of Different Devices, Using Techniques of Ionic Liquid Gating*. Université Grenoble Alpes, Grenoble, France, 2018.

[36] S. Sowmiah, V. Srinivasadesikan, M. C. Tseng, and Y. H. Chu, "On the chemical stabilities of ionic liquids," *Molecules*, vol. 14, no. 9. pp. 3780–3813, Sep. 2009, doi: 10.3390/molecules14093780.

[37] R. P. Swatloski, J. D. Holbrey, and R. D. Rogers, "Ionic liquids are not always green: Hydrolysis of 1-butyl-3-methylimidazolium hexafluorophosphate," *Green Chem.*, vol. 5, no. 4, pp. 361–363, 2003, doi: 10.1039/b304400a.

[38] B. Wang, W. Huang, L. Chi, M. Al-Hashimi, T. J. Marks, and A. Facchetti, "High-k gate dielectrics for emerging flexible and stretchable electronics," *Chem. Rev.*, vol. 118, no. 11, pp. 5690–5754, 2018, doi: 10.1021/acs.chemrev.8b00045.

[39] J. H. Cho *et al.*, "Printable ion-gel gate dielectrics for low-voltage polymer thin-film transistors on plastic," *Nat. Mater.*, vol. 7, no. 11, pp. 900–906, 2008, doi: 10.1038/nmat2291.

[40] B. Nketia-Yawson, A.-R. Jung, H. D. Nguyen, K.-K. Lee, B. Kim, and Y.-Y. Noh, "Difluorobenzothiadiazole and selenophene-based conjugated polymer demonstrating an effective hole mobility exceeding 5 cm^2 V^{-1} s^{-1} with solid-state electrolyte dielectric," *ACS Appl. Mater. Interfaces*, vol. 10, no. 38, pp. 32492–32500, Sep. 2018, doi: 10.1021/acsami.8b14176.

[41] J. Jeong *et al.*, "Ink-jet printable, self-assembled, and chemically crosslinked ion-gel as electrolyte for thin film, printable transistors," *Adv. Mater. Interfaces*, vol. 6, no. 21, Nov. 2019, Art. no. 1901074, doi: 10.1002/admi.201901074.

[42] Y. Ji, H. J. Lee, S. Lee, K. G. Cho, K. H. Lee, and K. Hong, "High-performance P-type copper(I) thiocyanate thin film transistors processed from solution at low temperature," *Adv. Mater. Interfaces*, vol. 6, no. 19, Oct. 2019, Art. no. 1900883, doi: 10.1002/admi.201900883.

[43] S. K. Lee, S. M. H. Kabir, B. K. Sharma, B. J. Kim, J. H. Cho, and J. H. Ahn, "Photo-patternable ion gel-gated graphene transistors and inverters on plastic," *Nanotechnology*, vol. 25, no. 1, p. 6, 2014, doi: 10.1088/0957-4484/25/1/014002.

[44] J. W. Park, C. Lee, and J. Jang, "High-performance field-effect transistor-type glucose biosensor based on nanohybrids of carboxylated polypyrrole nanotube wrapped graphene sheet transducer," *Sens. Actuators B, Chem.*, vol. 208, pp. 532–537, Mar. 2015, doi: 10.1016/j.snb.2014.11.085.

[45] K. G. Cho, Y. K. Cho, J. H. Kim, H. Y. Yoo, K. Hong, and K. H. Lee, "Thermostable ion gels for high-temperature operation of electrolyte-gated transistors," *ACS Appl. Mater. Interfaces*, vol. 12, no. 13, pp. 15464–15471, 2020, doi: 10.1021/acsami.9b23358.

[46] K. G. Cho, H. J. Kim, H. M. Yang, K. H. Seol, S. J. Lee, and K. H. Lee, "Sub-2 V, transfer-stamped organic/inorganic complementary inverters based on electrolyte-gated transistors," *ACS Appl. Mater. Interfaces*, vol. 10, no. 47, pp. 40672–40680, 2018, doi: 10.1021/acsami.8b13140.

[47] H. Y. Yoo *et al.*, "Tough and ionically conductive polymer electrolyte composites based on random copolymers with crystallizable side chain architecture," *Org. Electron.*, vol. 84, Sep. 2020, Art. no. 105788, doi: 10.1016/j.orgel.2020.105788.

[48] H. M. Yang, Y. K. Kwon, S. B. Lee, S. Kim, K. Hong, and K. H. Lee, "Physically cross-linked homopolymer ion gels for high performance electrolyte-gated transistors," *ACS Appl. Mater. Interfaces*, vol. 9, no. 10, pp. 8813–8818, 2017, doi: 10.1021/acsami.6b12283.

[49] Y. Na and F. S. Kim, "Nanodroplet-embedded semiconducting polymer layers for electrochemically stable and high-conductance organic electrolyte-gated transistors," *Chem. Mater.*, vol. 31, no. 13, pp. 4759–4768, 2019, doi: 10.1021/acs.chemmater.9b00995.

[50] S. H. Kim, K. Hong, K. H. Lee, and C. D. Frisbie, "Performance and stability of aerosol-jet-printed electrolyte-gated transistors based on poly(3-hexylthiophene)," *ACS Appl. Mater. Interfaces*, vol. 5, no. 14, pp. 6580–6585, 2013, doi: 10.1021/am401200y.

[51] J. H. Choi, W. Xie, Y. Gu, C. D. Frisbie, and T. P. Lodge, "Single ion conducting, polymerized ionic liquid triblock copolymer films: High capacitance electrolyte gates for N-type transistors," *ACS Appl. Mater. Interfaces*, vol. 7, no. 13, pp. 7294–7302, 2015, doi: 10.1021/acsami.5b00495.

[52] E. Said, X. Crispin, L. Herlogsson, S. Elhag, N. D. Robinson, and M. Berggren, "Polymer field-effect transistor gated via a poly(styrenesulfonic acid) thin film," *Appl. Phys. Lett.*, vol. 89, no. 14, 2006, Art. no. 143507, doi: 10.1063/1.2358315.

[53] Q. Thiburce and A. J. Campbell, "Low-voltage polyelectrolyte-gated polymer field-effect transistors gravure printed at high speed on flexible plastic substrates," *Adv. Electron. Mater.*, vol. 3, no. 2, 2016, Art. no. 1600421. doi: 10.1002/aelm.201600421.

[54] L. Herlogsson *et al.*, "Low-voltage polymer field-effect transistors gated via a proton conductor," *Adv. Mater.*, vol. 19, no. 1, pp. 97–101, Jan. 2007, doi: 10.1002/adma.200600871.

[55] H. Kim, B. J. Kim, Q. Sun, M. S. Kang, and J. H. Cho, "Graphene transistors gated by salted proton conductor," *Adv. Electron. Mater.*, vol. 2, no. 8, Aug. 2016, Art. no. 1600122, doi: 10.1002/aelm.201600122.

[56] Z. Liu, Z. Yin, J. Wang, and Q. Zheng, "Polyelectrolyte dielectrics for flexible low-voltage organic thin-film transistors in highly sensitive pressure sensing," *Adv. Funct. Mater.*, vol. 29, no. 1, pp. 1–11, 2019, doi: 10.1002/adfm.201806092.

[57] F. Von Seggern, I. Keskin, E. Koos, R. Kruk, H. Hahn, and S. Dasgupta, "Temperature-dependent performance of printed field-effect transistors with solid polymer electrolyte gating," *ACS Appl. Mater. Interfaces*, vol. 8, no. 46, pp. 31757–31763, 2016, doi: 10.1021/acsami.6b10939.

[58] K. Ton, A. Vighi, K. Lian, T.-Y. Chu, and Y. Tao, "Communication—Phosphoric acid based proton conducting polymer electrolytes for organic field effect transistor gate dielectrics," *ECS J. Solid State Sci. Technol.*, vol. 10, no. 5, 2021, Art. no. 055003, doi: 10.1149/2162-8777/abfa86.

[59] A. Virya and K. Lian, "A review of neutral pH polymer electrolytes for electrochemical capacitors: Transitioning from liquid to solid devices," *Mater. Rep. Energy*, vol. 1, no. 1, 2020, Art. no. 100005, doi: 10.1016/j.matre.2020.12.002.

[60] J. Li, J. Qiao, and K. Lian, "Hydroxide ion conducting polymer electrolytes and their applications in solid supercapacitors: A review," *Energy Storage Mater.*, vol. 24, pp. 6–21, Jan. 2020, doi: 10.1016/j.ensm.2019.08.012.

[61] D. E. Fenton, J. M. Parker, and P. V. Wright, "Complexes of alkali metal ions with poly(ethylene oxide)," *Polymer*, vol. 14, no. 11, p. 589, 1973, doi: 10.1016/0032-3861(73)90146-8.

[62] C. Samanta, R. R. Ghimire, and B. Ghosh, "Fabrication of amorphous indium-gallium-zinc-oxide thin-film transistor on flexible substrate using a polymer electrolyte as gate dielectric," *IEEE Trans. Electron Devices*, vol. 65, no. 7, pp. 2827–2832, Jul. 2018, doi: 10.1109/TED.2018.2834935.

[63] B. Wu *et al.*, "Multifunctional MoS2 transistors with electrolyte gel gating," *Small*, vol. 16, no. 22, Jun. 2020, Art. no. 2000420, doi: 10.1002/smll.202000420.

[64] B. Nasr, D. Wang, R. Kruk, H. Rösner, H. Hahn, and S. Dasgupta, "High-Speed, low-voltage, and environmentally stable operation of electrochemically gated zinc oxide nanowire field-effect transistors," *Adv. Funct. Mater.*, vol. 23, no. 14, pp. 1750–1758, 2013, doi: 10.1002/adfm.201202500.

[65] J. T. Carvalho *et al.*, "Fully printed zinc oxide electrolyte-gated transistors on paper," *Nanomaterials*, vol. 9, no. 2, p. 169, 2019, doi: 10.3390/nano9020169.

[66] S. Dasgupta, R. Kruk, N. Mechau, and H. Hahn, "Inkjet printed, high mobility inorganic-oxide field effect transistors processed at room temperature," *ACS Nano*, vol. 5, no. 12, pp. 9628–9638, 2011, doi: 10.1021/nn202992v.

[67] S. A. Singaraju *et al.*, "Development of fully printed electrolyte-gated oxide transistors using graphene passive structures," *ACS Appl. Electron. Mater.*, vol. 1, no. 8, pp. 1538–1544, 2019, doi: 10.1021/acsaelm.9b00313.

[68] G. C. Marques *et al.*, "Influence of humidity on the performance of composite polymer electrolyte-gated field-effect transistors and circuits," *IEEE Trans. Electron Devices*, vol. 66, no. 5, pp. 2202–2207, May 2019, doi: 10.1109/TED.2019.2903456.

[69] Y. He *et al.*, "Solution-processed natural gelatin was used as a gate dielectric for the fabrication of oxide field-effect transistors," *Org. Electron.*, vol. 38, pp. 357–361, Nov. 2016, doi: 10.1016/j.orgel.2016.09.017.

[70] I. Cunha *et al.*, "Reusable cellulose-based hydrogel sticker film applied as gate dielectric in paper electrolyte-gated transistors," *Adv. Funct. Mater.*, vol. 27, no. 16, Apr. 2017, Art. no. 1606755, doi: 10.1002/adfm.201606755.

[71] W. T. Gao, L. Q. Zhu, J. Tao, D. Y. Wan, H. Xiao, and F. Yu, "Dendrite integration mimicked on starch-based electrolyte-gated oxide dendrite transistors," *ACS Appl. Mater. Interfaces*, vol. 10, no. 46, pp. 40008–40013, 2018, doi: 10.1021/acsami.8b16495.

[72] N. Liu, L. Gan, Y. Liu, W. Gui, W. Li, and X. Zhang, "Improving pH sensitivity by field-induced charge regulation in flexible biopolymer electrolyte gated oxide transistors," *Appl. Surface Sci.*, vol. 419, pp. 206–212, Oct. 2017, doi: 10.1016/j.apsusc.2017.04.248.

[73] M. J. Panzer and C. D. Frisbie, "Polymer electrolyte-gated organic field-effect transistors: Low-voltage, high-current switches for organic electronics and testbeds for probing electrical transport at high charge carrier density," *J. Amer. Chem. Soc.*, vol. 129, no. 20, pp. 6599–6607, May 2007, doi: 10.1021/ja0708767.

[74] J. Pallu *et al.*, "A DNA hydrogel gated organic field effect transistor," *Org. Electron.*, vol. 75, Dec. 2019, Art. no. 105402, doi: 10.1016/j.orgel.2019.105402.

[75] X. Wang, L. Wei, P. Mou, F. Shao, and X. Gu, "A printable GO-PVA composite dielectric for EDL gating of metal-oxide TFTs," *Flexible Printed Electron.*, vol. 5, no. 1, 2020, Art. no. 015002, doi: 10.1088/2058-8585/ab603c.

[76] C. V. Chaparro, L. V. Herrera, A. M. Meléndez, and D. A. Miranda, "Considerations on electrical impedance measurements of electrolyte solutions in a four-electrode cell," *J. Phys. Conf. Series*, vol. 687, no. 1, 2016, Art. no. 012101, doi: 10.1088/1742-6596/687/1/012101.

[77] T. Sato, G. Masuda, and K. Takagi, "Electrochemical properties of novel ionic liquids for electric double layer capacitor applications," *Electrochimica Acta*, vol. 49, no. 21, pp. 3603–3611, 2004, doi: 10.1016/j.electacta.2004.03.030.

[78] R. Yang, S. Zhang, L. Zhang, and X. Bi, "Effects of LiClO4 on the characteristics and ionic conductivity of the solid polymer electrolytes composed of PEO, LiClO4 and PLiAA," in *Proc. Mater. Sci. Forum*, 2013, pp. 53–58, doi: 10.4028/www.scientific.net/MSF.743-744.53.

[79] C. Sun *et al.*, "Facile and cost-effective liver cancer diagnosis by water-gated organic field-effect transistors," *Biosens. Bioelectron.*, vol. 164, Sep. 2020, Art. no. 112251, doi: 10.1016/j.bios.2020.112251.

[80] E. Macchia *et al.*, "Selective single-molecule analytical detection of C-reactive protein in saliva with an organic transistor," *Anal. Bioanal. Chem.*, vol. 411, no. 19, pp. 4899–4908, 2019, doi: 10.1007/s00216-019-01778-2.

[81] T. T. K. Nguyen *et al.*, "Triggering the electrolyte-gated organic field-effect transistor output characteristics through gate functionalization using diazonium chemistry: Application to biodetection of 2,4-dichlorophenoxyacetic acid," *Biosens. Bioelectron.*, vol. 113, pp. 32–38, Aug. 2018, doi: 10.1016/j.bios.2018.04.051.

[82] M. Y. Mulla *et al.*, "Capacitance-modulated transistor detects odorant binding protein chiral interactions," *Nat. Commun.*, vol. 6, p. 6010, Jan. 2015, doi: 10.1038/ncomms7010.

[83] E. Piccinini, C. Bliem, C. Reiner-Rozman, F. Battaglini, O. Azzaroni, and W. Knoll, "Enzyme-polyelectrolyte multilayer assemblies on reduced graphene oxide field-effect transistors for biosensing applications," *Biosens. Bioelectron.*, vol. 92, pp. 661–667, Jun. 2017, doi: 10.1016/j.bios.2016.10.035.

[84] A. Kyndiah *et al.*, "Bioelectronic recordings of cardiomyocytes with accumulation mode electrolyte gated organic field effect transistors," *Biosens. Bioelectron.*, vol. 150, Feb. 2020, Art. no. 111844, doi: 10.1016/j.bios.2019.111844.

[85] F. Scuratti *et al.*, "Real-time monitoring of cellular cultures with electrolyte-gated carbon nanotube transistors," *ACS Appl. Mater. Interfaces*, vol. 11, no. 41, pp. 37966–37972, 2019, doi: 10.1021/acsami.9b11383.

[86] M. Zhang, C. Liao, C. H. Mak, P. You, C. L. Mak, and F. Yan, "Highly sensitive glucose sensors based on enzyme-modified whole-graphene solution-gated transistors," *Sci. Rep.*, vol. 5, p. 8311, Feb. 2015, doi: 10.1038/srep08311.

[87] Q. Liu *et al.*, "Highly sensitive and wearable In_2O_3 nanoribbon transistor biosensors with integrated on-chip gate for glucose monitoring in body fluids," *ACS Nano*, vol. 12, no. 2, pp. 1170–1178, 2018, doi: 10.1021/acsnano.7b06823.

[88] D. H. Shin, W. Kim, J. Jun, J. S. Lee, J. H. Kim, and J. Jang, "Highly selective FET-type glucose sensor based on shape-controlled palladium nanoflower-decorated graphene," *Sens. Actuators B, Chem.*, vol. 264, pp. 216–223, Jul. 2018, doi: 10.1016/j.snb.2018.02.139.

[89] M. Fathollahzadeh *et al.*, "Immobilization of glucose oxidase on ZnO nanorods decorated electrolyte-gated field effect transistor for glucose detection," *J. Solid State Electrochem.*, vol. 22, no. 1, pp. 61–67, 2018, doi: 10.1007/s10008-017-3716-y.

[90] K. S. Bhat, R. Ahmad, J. Y. Yoo, and Y. B. Hahn, "Nozzle-jet printed flexible field-effect transistor biosensor for high performance glucose detection," *J. Colloid Interface Sci.*, vol. 506, pp. 188–196, Nov. 2017, doi: 10.1016/j.jcis.2017.07.037.

[91] Y. Huang, X. Dong, Y. Shi, C. M. Li, L. J. Li, and P. Chen, "Nanoelectronic biosensors based on CVD grown graphene," *Nanoscale*, vol. 2, no. 8, pp. 1485–1488, 2010, doi: 10.1039/c0nr00142b.

[92] C. Huang, Z. Hao, T. Qi, Y. Pan, and X. Zhao, "An integrated flexible and reusable graphene field effect transistor nanosensor for monitoring glucose," *J. Mater.*, vol. 6, no. 2, pp. 308–314, 2020, doi: 10.1016/j.jmat.2020.02.002.

[93] E. W. Nery, M. Kundys, P. S. Jeleń, and M. Jönsson-Niedziólka, "Electrochemical glucose sensing: Is there still room for improvement?" *Anal. Chem.*, vol. 88, no. 23, pp. 11271–11282, 2016, doi: 10.1021/acs.analchem.6b03151.

[94] E. H. Yoo and S. Y. Lee, "Glucose biosensors: An overview of use in clinical practice," *Sensors*, vol. 10, no. 5, pp. 4558–4576, 2010, doi: 10.3390/s100504558.

[95] J. R. Sempionatto, J.-M. Moon, and J. Wang, "Touch-based fingertip blood-free reliable glucose monitoring: Personalized data processing for predicting blood glucose concentrations," *ACS Sens.*, 2021, doi: 10.1021/acssensors.1c00139. [Online]. Available: https://pubs.acs.org/doi/10.1021/acssensors.1c00139

[96] C. Tack *et al.*, "Accuracy evaluation of five blood glucose monitoring systems obtained from the pharmacy: A European multicenter study with 453 subjects," *Diabetes Technol. Ther.*, vol. 14, no. 4, pp. 330–337, 2012, doi: 10.1089/dia.2011.0170.

[97] H. J. Jang *et al.*, "Electronic cortisol detection using an antibody-embedded polymer coupled to a field-effect transistor," *ACS Appl. Mater. Interfaces*, vol. 10, no. 19, pp. 16233–16237, 2018, doi: 10.1021/acsami.7b18855.

[98] K. H. Kim, S. H. Lee, S. E. Seo, J. Bae, S. J. Park, and O. S. Kwon, "Ultrasensitive stress biomarker detection using polypyrrole nanotube coupled to a field-effect transistor," *Micromachines*, vol. 11, no. 4, p. 439, 2020, doi: 10.3390/MI11040439.

[99] G. Jeong, J. Oh, and J. Jang, "Fabrication of N-doped multidimensional carbon nanofibers for high-performance cortisol biosensors," *Biosens. Bioelectron.*, vol. 131, pp. 30–36, Apr. 2019, doi: 10.1016/j.bios.2019.01.061.

[100] R. Massey, S. Bebe, and R. Prakash, "Aptamer-Enhanced organic electrolyte-gated FET biosensor for high-specificity detection of cortisol," *IEEE Sensors Lett.*, vol. 4, no. 7, Jul. 2020, Art. no. 4500604. [Online]. Available: https://ieeexplore.ieee.org/stamp/stamp.jsp?tp=&arnumber=9117013

[101] S. Veeralingam and S. Badhulika, "Surface functionalized β-Bi2O3 nanofibers based flexible, field-effect transistor-biosensor (BioFET) for rapid, label-free detection of serotonin in biological fluids," *Sens. Actuators B, Chem.*, vol. 321, Oct. 2020, Art. no. 128540, doi: 10.1016/j.snb.2020.128540.

[102] S. Casalini, F. Leonardi, T. Cramer, and F. Biscarini, "Organic field-effect transistor for label-free dopamine sensing," *Org. Electron.*, vol. 14, no. 1, pp. 156–163, 2013, doi: 10.1016/j.orgel.2012.10.027.

[103] M. Zhang, C. Liao, Y. Yao, Z. Liu, F. Gong, and F. Yan, "High-performance dopamine sensors based on whole-graphene solution-gated transistors," *Adv. Funct. Mater.*, vol. 24, no. 7, pp. 978–985, 2014, doi: 10.1002/adfm.201302359.

[104] V. D. Bhatt, S. Joshi, M. Becherer, and P. Lugli, "Flexible, low-cost sensor based on electrolyte gated carbon nanotube field effect transistor for organo-phosphate detection," *Sensors*, vol. 17, no. 5, p. 1147, 2017, doi: 10.3390/s17051147.

[105] G. E. Fenoy, W. A. Marmisollé, O. Azzaroni, and W. Knoll, "Acetylcholine biosensor based on the electrochemical functionalization of graphene field-effect transistors," *Biosens. Bioelectron.*, vol. 148, Jan. 2020, Art. no. 111796, doi: 10.1016/j.bios.2019.111796.

[106] Y. Liu, B. Li, L. Zhu, P. Feng, Y. Shi, and Q. Wan, "Dopamine detection based on low-voltage oxide homojunction electric-double-layer thin-film transistors," *IEEE Electron Device Lett.*, vol. 37, no. 6, pp. 778–781, Jun. 2016, doi: 10.1109/LED.2016.2560201.

[107] I. Gualandi, D. Tonelli, F. Mariani, E. Scavetta, M. Marzocchi, and B. Fraboni, "Selective detection of dopamine with an all PEDOT: PSS Organic electrochemical Transistor," *Sci. Rep.*, vol. 6, Oct. 2016, Art. no. 35419, doi: 10.1038/srep35419.

[108] C. Liao, M. Zhang, L. Niu, Z. Zheng, and F. Yan, "Organic electrochemical transistors with graphene-modified gate electrodes for highly sensitive and selective dopamine sensors," *J. Mater. Chem. B*, vol. 2, no. 2, pp. 191–200, 2014, doi: 10.1039/c3tb21079k.

[109] X. Qing *et al.*, "Wearable fiber-based organic electrochemical transistors as a platform for highly sensitive dopamine monitoring," *ACS Appl. Mater. Interfaces*, vol. 11, no. 14, pp. 13105–13113, 2019, doi: 10.1021/acsami.9b00115.

[110] R. Massey, E. Morin, M. C. DeRosa, and R. Prakash, "Label-free detection of dopamine using aptamer enhanced organic-electrolyte gated FET sensor," in *Proc. IEEE Int. Conf. Flex. Printable Sens. Syst.*, 2019, pp. 2019–2021, doi: 10.1109/FLEPS.2019.8792324.

[111] S. P. White, S. Sreevatsan, C. D. Frisbie, and K. D. Dorfman, "Rapid, selective, label-free aptameric capture and detection of ricin in potable liquids using a printed floating gate transistor," *ACS Sens.*, vol. 1, no. 10, pp. 1213–1216, Oct. 2016, doi: 10.1021/acssensors.6b00481.

[112] S. T. Le *et al.*, "Quantum capacitance-limited MoS2 biosensors enable remote label-free enzyme measurements," *Nanoscale*, vol. 11, no. 33, pp. 15622–15632, Sep. 2019, doi: 10.1039/c9nr03171e.

[113] Q. Zhang, F. Leonardi, S. Casalini, I. Temiño, and M. Mas-Torrent, "High performing solution-coated electrolyte-gated organic field-effect transistors for aqueous media operation," *Sci. Rep.*, vol. 6, pp. 1–10, Dec. 2016, doi: 10.1038/srep39623.

[114] K. Alexandrou, N. Petrone, J. Hone, and I. Kymissis, "Encapsulated graphene field-effect transistors for air stable operation," *Appl. Phys. Lett.*, vol. 106, no. 11, 2015, Art. no. 113104, doi: 10.1063/1.4915513.

[115] M. Robin *et al.*, "Overcoming electrochemical instabilities of printed silver electrodes in all-printed ion gel gated carbon nanotube thin-film transistors," *ACS Appl. Mater. Interfaces*, vol. 11, no. 44, pp. 41531–41543, 2019, doi: 10.1021/acsami.9b14916.

[116] G. C. Marques *et al.*, "Electrolyte-gated FETs based on oxide semiconductors: Fabrication and modeling," *IEEE Trans. Electron Devices*, vol. 64, no. 1, pp. 279–285, Jan. 2017, doi: 10.1109/TED.2016.2621777.

[117] C. H. Kim *et al.*, "A compact model for organic field-effect transistors with improved output asymptotic behaviors," *IEEE Trans. Electron Devices*, vol. 60, no. 3, pp. 1136–1141, Mar. 2013, doi: 10.1109/TED.2013.2238676.

[118] F. Hain, M. Graef, B. Iñíguez, and A. Kloes, "Charge based, continuous compact model for the channel current in organic thin-film transistors for all regions of operation," *Solid. State. Electron.*, vol. 133, pp. 17–24, Jul. 2017, doi: 10.1016/j.sse.2017.04.002.

[119] F. Rasheed, M. Hefenbrock, M. Beigl, M. B. Tahoori, and J. Aghassi-Hagmann, "Variability modeling for printed inorganic electrolyte-gated transistors and circuits," *IEEE Trans. Electron Devices*, vol. 66, no. 1, pp. 146–152, Jan. 2019, doi: 10.1109/TED.2018.2867461.

[120] G. C. Marques, D. Weller, A. T. Erozan, X. Feng, M. Tahoori, and J. Aghassi-Hagmann, "Progress report on 'from printed electrolyte-gated metal-oxide devices to circuits,'" *Adv. Mater.*, vol. 31, no. 26, 2019, Art. no. 1806483, doi: 10.1002/adma.201806483.

[121] Y. Xia *et al.*, "Printed sub-2 V Gel-electrolyte-gated polymer transistors and circuits," *Adv. Funct. Mater.*, vol. 20, no. 4, pp. 587–594, 2010, doi: 10.1002/adfm.200901845.